Analysis of Post-Weld Deformation at the Heat-Affected Zone Using External Forces Based on the Inherent Strain

Yun Sok Ha[1,#], Chang Doo Jang[2], Jong Tae Kim[2] and Hyung Suk Mun[3]

1 Welding Research Part ,SAMSUNG HEAVY INDUSTRIES CO., LTD. GEOJE SHIPYARD 530, Jangpyeong-Ri, Sinhyeon-Eup, Geoje-Si, South Korea, 656-710
2 Dept. of Naval Architecture and Ocean Engineering, Seoul National University San 56-1, Sillim-Dong, Kwanak-Gu, Seoul, South Korea, 151-744
3 Railway System & Safety Research Dept, Korea Railroad Research Institute, Woram-Dong, Uiwang-Si, Gyeonggi, South Korea, 437-757
Corresponding Author / E-mail: hsmun@krri.re.kr, TEL: +82-31-460-5682, FAX: +82-31-460-5699

KEYWORDS : Equivalent loading method, Hardening, Inherent strain, Residual stress, Welding distortion

An analytical method to predict the post-weld deformation at the heat-affected zone (HAZ) is presented in this paper. The method was based on the assumption that the post-weld deformation is caused by external forces resulting from the inherent strain, which is defined as the irrecoverable strain after removing structural restraints and loadings. In general, the equivalent loading method can be used to analyze distortions in welding areas because it is efficient and effective. However, if additional loads are applied after welding, it is difficult to determine the final strain on a welded structure. To determine the final strain of a welded structure at the HAZ more accurately, we developed a modified equivalent loading method based on the inherent strain that incorporated hardening effects. The proposed method was applied to calculate the residual stress at the HAZ. Experiments were also conducted on welded plates to evaluate the validity of the proposed method.

Manuscript received: March 14, 2007 / Accepted: August 24, 2007

NOMENCLATURE

B = breadth of the specimen
b = maximum breadth of the inherent strain region
d = maximum depth of the inherent strain region
D = deformation at the center
E = tangent modulus of the level lower than the yielding point
Et = tangent modulus of the level higher than the yielding point
E_1 = Young's modulus of the temperature change region (Young's modulus of the disk)
E_2 = Young's modulus of the adjacent region (Young's modulus of the plate)
H = hardening coefficient (N/m^2)
h = thickness of the plate
k_1 = thermal conductivity coefficient of the temperature change region
k_2 = thermal conductivity coefficient of the adjacent region
m_y = moment on the welded line (Equivalent load)
v = Poisson's ratio
v_1 = Poisson ratio of the temperature change region
v_2 = Poisson ratio of the adjacent region
Z = section modulus
α = thermal coefficient (1/℃)
ε = total strain
ε^e = elastic strain
ε^p = plastic strain
ε^{th} = thermal strain
ε^{tr} = phase transformation strain
ε^* = inherent strain
ε^*_L = inherent strain generated by the loading condition
ε^*_{UL} = inherent strain generated by the unloading condition
σ_p = stress incremental
σ_R = residual stress
σ_Y = yield stress

1. Introduction

Shipbuilding involves many welded structures. Welding is the most important aspect of shipbuilding since it is used to permanently join two metal parts. During the welding process, heat (and sometimes pressure) is applied to two metal pieces to form a permanent bond between them. Extending the life of a product requires enhancing the quality and durability of its welded parts.

The welding process is subject to certain problems related to the deformation of materials by heat, phase transformations, residual stresses, and welding defects. In particular, the deformation that occurs during the heating and cooling processes of welding operations significantly affects the required precision and stability of structural materials. Also, when a welded zone is subject to additional

loads, the deformation generated by the residual stresses differs from the deformation of a material in elastic conditions. Therefore, accurate analyses require predictions of the deformation generated by the additional loads in a welded zone.

Among the methods used to predict welding deformations, the equivalent loading method based on the inherent strain (Jang *et al.*[1]) has been successfully used for the last ten years due to its effective and reliable results. It is important to determine the inherent strain regions. The inherent strain method does this by calculating the temperature distribution during welding (Jang *et al.*[2]) and converting it into equivalent loads, from which it is able to determine the deformation. Because this method independently generates a term related to the angular deformation, it can be applied very efficiently to precision deformation processes, which are sensitive to phase transformations such as line heating (Ha and Jang[3]).

The method developed in this study also incorporates the hardening of metal. Conventional studies of heat-affected zone (HAZ) deformation have assumed that the residual stress in plastic regions is equal to the yield stress. It is therefore difficult to estimate the deformation when additional loads are added to post-deformation parts. However, a method that incorporates hardening can predict this deformation because it can define the stress levels over the yield stress. We developed such a model and compared our analysis results with experimental data to validate its usefulness and effectiveness.

2. Inherent strain in the HAZ

The total strain can be divided into the elastic, thermal, plastic, and phase transformation strains,

$$\varepsilon = \varepsilon^{th} + \varepsilon^{p} + \varepsilon^{tr} + \varepsilon^{e} \tag{1}$$

The inherent strain is defined as the irrecoverable strain after removing structural restraints and loads, or the sum of elastically irrecoverable strains that induce permanent deformation of the material,

$$\varepsilon^{*} = \varepsilon^{th} + \varepsilon^{p} + \varepsilon^{tr} = \varepsilon - \varepsilon^{e} \tag{2}$$

Typical inherent strains include plastic, thermal, and phase transformation strains, *i.e.*, the total strain with the exception of the elastic strain (Ha and Jang[3]).

A one-dimensional (1D) bar-spring model (Fig. 1) can be used to define the welded zone and the inherent strain caused by welding (Jang *et al.*[4]). The bar in Fig. 1 represents the temperature change region while the spring in represents the area of the welded zone with the exception of the temperature change region. Using a similar method, Fig. 2 uses a two-dimensional (2D) plate-spring model to describe the welded zone conditions in more detail. The 2D plate-spring model applies the coefficient and spring constant from the 1D bar spring model. The spring model simulates the elastic restraint from the surrounding area outside the disk against the disk expansion and shrinkage caused by a temperature change. During temperature changes, the spring's restraining action induces an internal stress in the bar. The inherent strain equation,

$$\varepsilon^{*} = -\frac{\sigma_Y}{E_1}\left(\frac{k_1}{k_2}+1\right) \qquad \left[\because k_1 = \frac{AE_1}{L}\right] \tag{3}$$

where

$$k_1 = \frac{E_1}{r(1-\nu_1)}, \quad k_2 = \frac{E_2}{r(1+\nu_2)} \tag{4}$$

and the equilibrium force equation,

$$k_2 \cdot x = -\sigma_Y \cdot A \tag{5}$$

determine the final inherent strain in the disk spring.

$$\varepsilon^{*} = -\frac{\sigma_Y}{E_1}\left(\frac{E_1}{E_2}\cdot\frac{1+\nu_1}{1-\nu_2}+1\right) \tag{6}$$

Equation 5 indicates that the external force acting on a bar by a spring equals a material's internal force. Based on the definition of the spring constants in Eq. 4, the 2D plate-spring model expresses the inherent strain as given by Eq. 6.

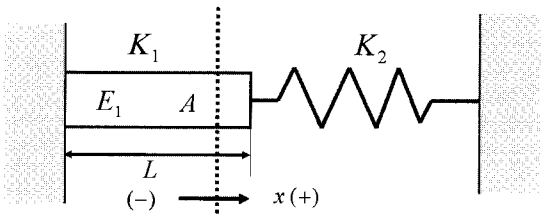

Fig. 1 Force equilibrium in bar-spring model

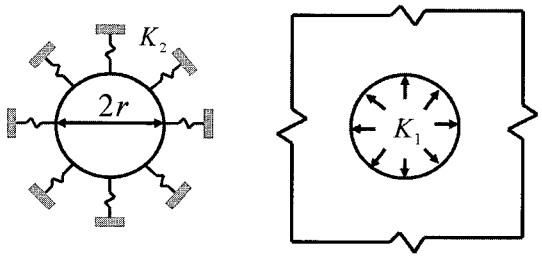

Fig. 2 Force equilibrium in disk-spring model

Figure 3 presents a normal stress – strain diagram. In this figure, the residual stress acting on the material does not incorporate hardening effects. Therefore, its stress level is always equal to the yield stress, $\sigma_Y = \sigma_R$. Point A in Fig. 3 indicates the initial location of the yield stress. The conventional inherent strain method only considers the normal stress. Therefore, if an inherent strain model can incorporate hardening effects, it will produce more reliable results.

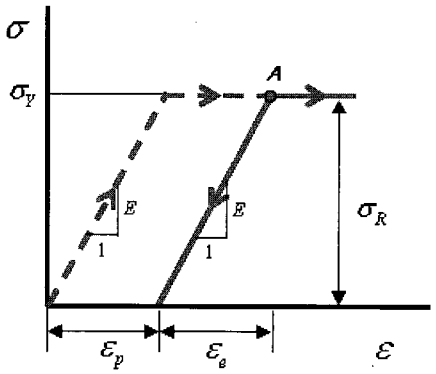

Fig. 3 Yield state material on elastic-perfect plastic stress-strain relation curve

3. Inherent strain that incorporates hardening

The stress – strain diagram in Fig. 4 shows the additional stress caused by the hardening effects. Point A in Fig. 4 indicates the material status after the yield stress is reached. Due to the additional hardening effects, the level of the residual stress shown in Fig. 4 is always higher than that of the residual stress shown in Fig. 3.

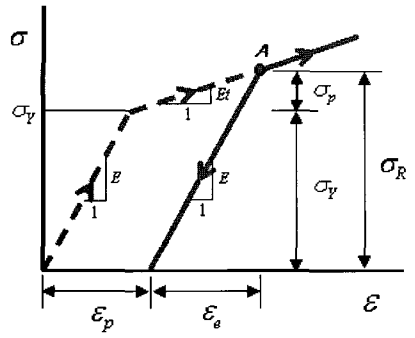

Fig. 4 Yield state material on elastic-plastic stress-strain relation curve

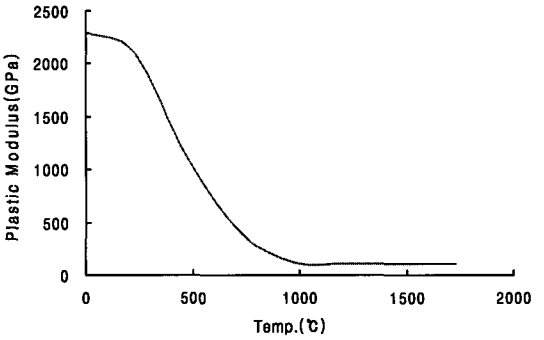

Fig. 5 Et(tangential modulus) of low carbon steel (Patel^5)

If a strain-stress diagram incorporates the hardening effects, the stress increment must be included after the yielding process. Thus, the total residual stress can be defined as the sum of the yield stress (σ_y) and stress increment (σ_P). The stress increment is equal to the plastic stress, predicted by the hardening coefficient (H) that is described in greater detail in Section 4. When the plastic stress is added to Eq. 5, it results in

$$k_2 \cdot x = -(\sigma_Y + \sigma_P) \cdot A \tag{7}$$

$$x = -\frac{(\sigma_Y + \sigma_P) \cdot A}{k_2} \tag{8}$$

The hardening coefficient can then be substituted,

$$\varepsilon^* = -\frac{\sigma_Y + \sigma_P}{E_1}\left(\frac{k_1}{k_2} + 1\right) = -\frac{\sigma_Y + H \cdot \varepsilon^p}{E_1}\left(\frac{k_1}{k_2} + 1\right) \quad \left[\because \sigma_P = H \cdot \varepsilon^p\right] \tag{9}$$

If the phase transformation (ε^{tr}) is neglected or included in the thermal strain term (ε^{tr}) in Eq. 2, then

$$\varepsilon^* = \varepsilon^{th} + \varepsilon^p \quad \Rightarrow \quad \varepsilon^p = \varepsilon^* - \varepsilon^{th} \tag{10}$$

After substituting Eq. 10 into Eq. 9, the equation of the inherent strain incorporating hardening is

$$\varepsilon^* = -\frac{\sigma_Y + H \cdot (\varepsilon^* - \varepsilon^{th})}{E_1}\left(\frac{k_1}{k_2} + 1\right) \tag{11}$$

The inherent strain including hardening (ε^*) appears on both sides of Eq. 11. This can be rewritten as follows:

$$\varepsilon^* = \frac{-\sigma_Y + H \cdot \int \alpha \, dT}{E_1 + H \cdot \left(\frac{k_1}{k_2} + 1\right)}\left(\frac{k_1}{k_2} + 1\right) \quad \left[\because \varepsilon^{th} = \int \alpha \, dT\right] \tag{12}$$

4. Determining the hardening coefficient

Figure 5 shows the plastic modulus – temperature diagram introduced by Patel[5]. It can be applied to determine the hardening coefficient of mild steel (carbon $\leq$ 0.3%). The plastic modulus E is related to the hardening coefficient H by

$$H = \frac{E \cdot Et}{E - Et} \tag{13}$$

where Et is a temperature-dependent material variable that is used to determine the inherent strain considering hardening (ε^*).

5. Determining the residual stress based on the inherent strain

The residual stress is the sum of the yield and plastic stresses,

$$\sigma_R = \sigma_Y + \sigma_P \tag{14}$$

Substituting Eq. 14 into Eq. 9 yields

$$\varepsilon^* = -\frac{\sigma_R}{E_1}\left(\frac{k_1}{k_2} + 1\right) \tag{15}$$

Substituting Eq. 15 into Eq. 12 gives

$$\sigma_R = \frac{E_1(\sigma_Y - H \cdot \int \alpha \, dT)}{E_1 + H\left(\frac{k_1}{k_2} + 1\right)} \tag{16}$$

which gives the residual stress under unusual circumstances, known as the restricted HAZ.

6. Deformation experiment using a flat plate

A bead-on-plate welding specimen was prepared to verify the expressions for the inherent strain including the hardening effects (Eq. 12) and the residual stress under unusual circumstances (Eq. 15). The experiment was conducted according to ship classification standards. The dimensions of the specimen are given in Fig. 6.

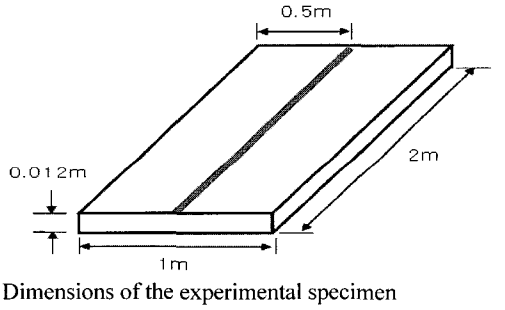

Fig. 6 Dimensions of the experimental specimen

The following procedure was followed during the experiment.

(1). Bead-on-plate welding was performed in the middle of the specimen in the length-wise direction.
(2). The angle deformation from welding was measured in the breadth-wise direction after the specimen was cooled.
(3). The plate was turned over.
(4). An additional load (140 kg) was added to the center of the plate and then removed.
(5). The plate deformation was measured.

Care was taken to avoid generating additional residual stresses by applying the heavy overload during Step 4.

The conventional inherent strain equation can only predict the welding deformation. If an additional load is applied to the welded joints, this method is unable to calculate the total deformation by incorporating the hardening effects. When an additional load is added or removed from a specimen, it is difficult for the conventional inherent strain method to predict the variation of strain because it only considers internal stresses, which always equal yield stress. Therefore, the conventional equation of inherent strain cannot predict stress deformations greater than the yield stress.

In contrast, an inherent strain equation that incorporates the hardening effects can predict the deformation of the structure receiving the additional load after welding. This is particularly relevant to shipbuilding, because ship structures are subject to various loads after welding, such as additional welding, lifting, transportation, docking, *etc.*

7. Deformation analysis and introduction of the equivalent loading method

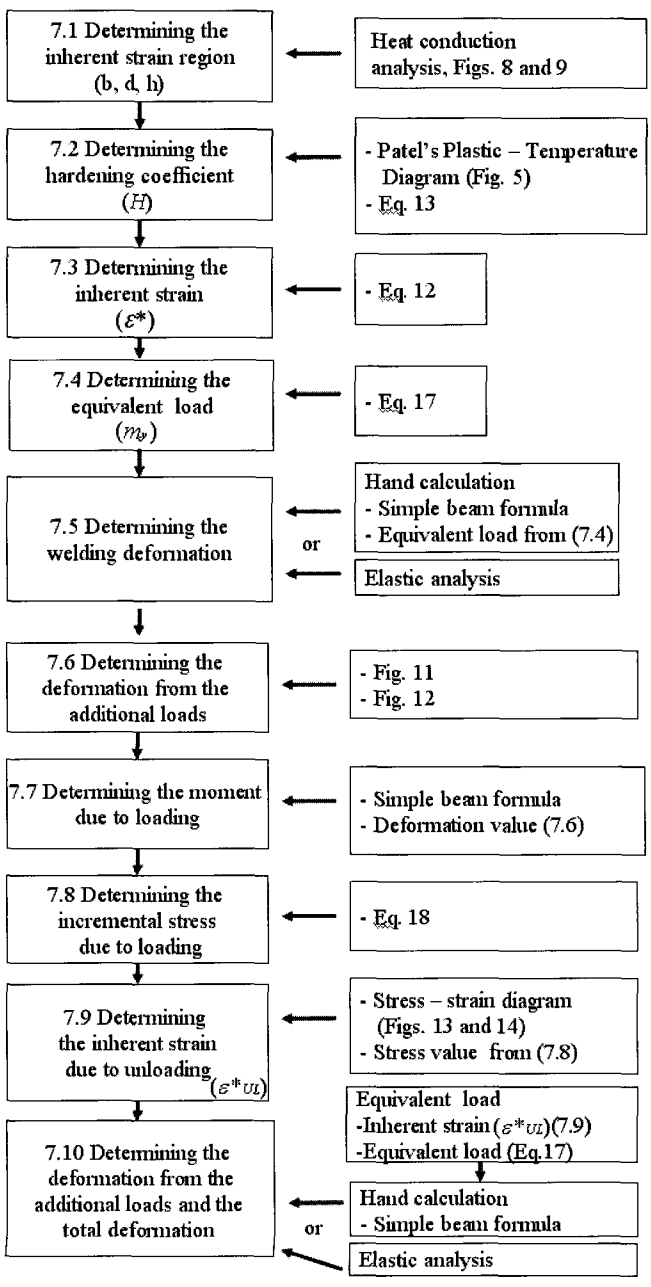

Fig. 7 Flowchart of developed post-weld distortion analysis

Figure 7 shows a flow diagram of the deformation analysis process. Only the process from Sections 7.1 to 7.5 is related to the welding deformation analysis that includes the hardening effects.

7.1 Determining the inherent strain region

First, a heat conduction analysis was performed to determine the inherent strain region. The analysis was based on the assumption that a metallurgical phase is transformed into an austenite state (AC1), and applied a standard methodology to determine the inherent strain region (Ha and Jang[3]).

Two-dimensional modeling was used for the computational heat conduction analysis, as shown in Fig. 8. The bead was modeled bead separately from the plate for the bead-on-plate welding analysis, and an initial temperature of 2300°C was applied to the bead (Lee *et al.*[6]). Any area reaching temperatures above 700°C during the welding process was defined as part of the inherent strain region (Ko *et al.*[7]). Figure 9 shows the maximum breath (a) and maximum depth (b) of the inherent strain region. The geometry of the inherent strain region within the experimental welding plate is illustrated in Fig. 9(c).

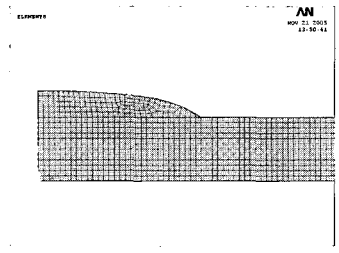

Fig. 8 Heat transfer model of bead-on plate welding

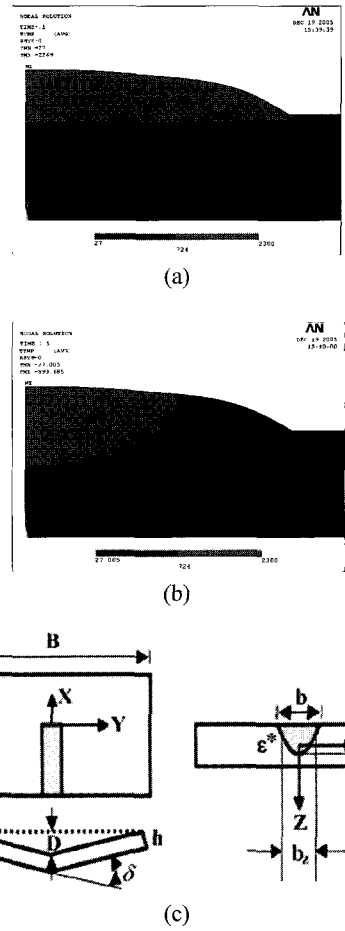

Fig. 9 Heat transfer analysis and geometry of the inherent strain region

7.2 Determining the hardening coefficient

The hardening coefficient was determined as discussed in Section 4.

7.3 Determining the inherent strain

The inherent strain was determined using Eq. 12 based on the value of H.

7.4 Determining the equivalent load

The inherent strain was converted into an equivalent load by substituting the values determined in Sections 7.1 and 7.3 into the following equation (Ko *et al.*[7]):

$$m_y = \frac{1}{6} E_1 \varepsilon^* dh \left(\frac{3\pi}{4} - 2\frac{d}{h}\right) \tag{17}$$

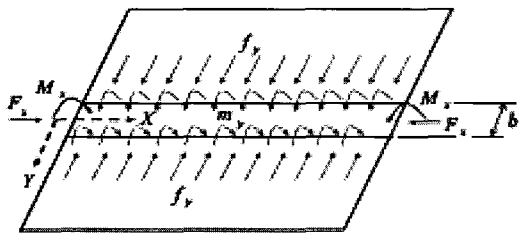

Fig. 10 Distribution of the equivalent load along the welded line equation (Ko *et al.*[7])

7.5 Determining the welding deformation

The welding deformation of the specimen can be calculated using the elastic analysis method introduced by Jang *et al.*[1] and Nomoto *et al.*[8] It can also be calculated using a simple beam deflection formula, as described in Sections 7.5 and 7.10.

7.6 Determining the deformation from the additional loads

The gravity of steel (7.83 kg/mm^3) was converted to a uniform load and applied to this specific example, as shown in Fig. 11. The uniform distributed load along the welded line was defined as the additional load generating the deformation (see Fig. 12). This load was applied to the specific example and the resulting deformation was measured.

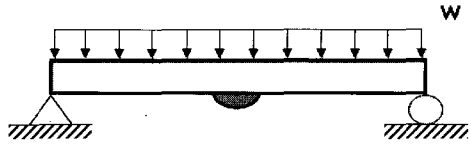

Fig. 11 Free body diagram showing the weight of the plate after it is turned over

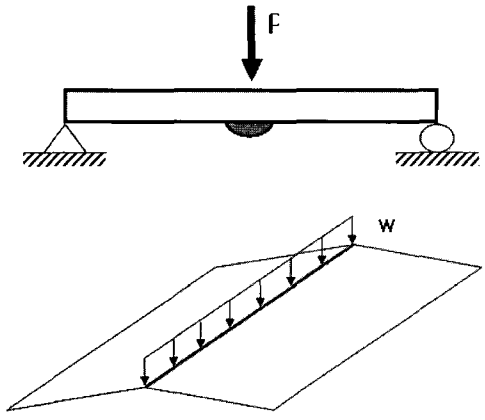

Fig. 12 Determining the effects of loading and unloading

7.7 Determining the moment due to loading

The moment acting on the welding point due to the additional loading M was calculated using a simple beam deflection formula and the value of the deformation (see Section 7.6).

7.8 Determining the incremental stress due to loading

The incremental stress was obtained from

$$\sigma = \frac{M}{Z} \tag{18}$$

and was used to determine the level of point B shown in the stress – strain diagram given in Fig. 13.

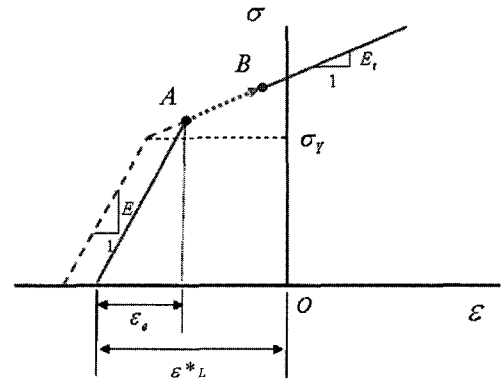

Fig. 13 Loading process

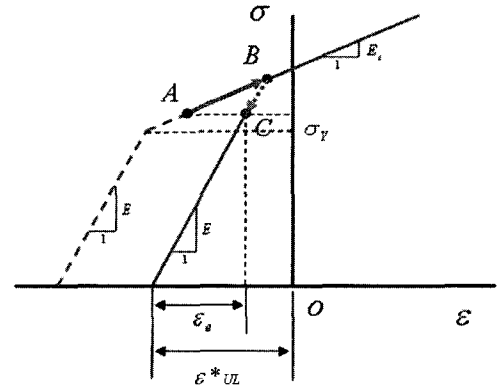

Fig. 14 Unloading process

7.9 Determining the strain due to unloading

The strain generated from the additional loads can be defined using the stress – strain diagram that includes the hardening effects. Figures 13 and 14 show the relationship between the stress and strain in the HAZ. Point 'A' represents the conditions after welding. When incorporating the hardening effects, if an additional load is applied to a specimen, point 'A' moves toward point 'B' to a degree equal to the stress increment. After the load is removed, point 'B' moves toward point 'C'. The inherent strain shown in Fig. 13 (ε^*_L) and Fig. 14 (ε^*_{UL}) decreased during the loading and unloading process. However, the residual stress did not increase from point 'A' to point 'C'. Therefore, if Eq. 18 determines the incremental stress at the welding point under an additional load, the stress – strain diagram can predict the minimum value of the inherent strain while considering the hardening effects.

7.10 Determining the deformation from the additional loads and the total deformation

The inherent strain generated under loading and unloading conditions can be determined by the stress – strain diagram (see Fig. 14). The value of ε^*_{UL} enables us to calculate the total deformation of the welded joint after an additional loading and unloading. The equivalent load can be determined by substituting the value of ε^*_{UL} and the geometric value of the inherent strain regions (see Section 7.1) into Eq. 17. The total deformation is calculated

using the deformation analysis process (see Section 7.5). Finally, the processes described in sections 7.4 and 7.5 (equivalent loading method based on the inherent strain) can be repeated to determine the total deformation during the process.

Table 1 Comparison of the experimental results with the maximum distortion analysis

	Welding deformation (mm)	Deformation after loading and removing the additional load (mm)
Experimental results (1)	8.69	7.92
Analysis results using the proposed ε^* (2)	8.51	7.67
Analysis results using the conventional ε^* (3)	8.29	-
Comparison of (1)/(2)	1.02	1.03
Comparison of (1)/(3)	1.05	-

Table 1 gives the maximum deformation calculated from the experiment and the analyses measured at the central point of the specimen in the direction of its breadth. The results of the proposed method were closer to the experimental values than those of the conventional method. While the conventional method (see Fig. 15) was able to predict the welding deformation, it was limited because it could not incorporate additional loads after welding.

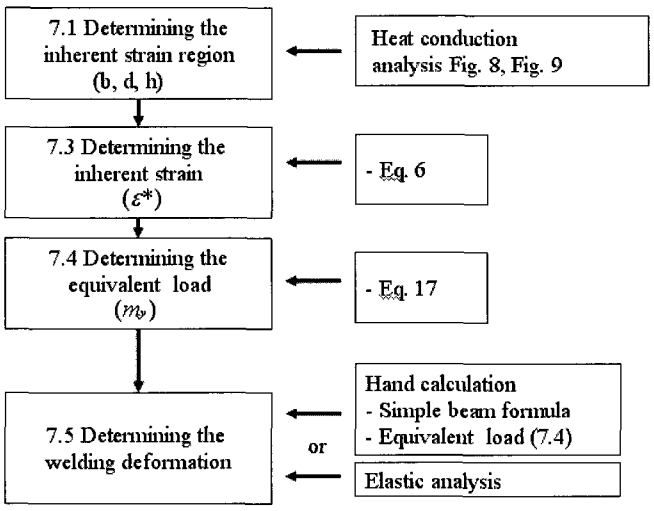

Fig. 15 Conventional deformation analysis process

8. Conclusions

We developed a new method for calculating the inherent strain by incorporating the hardening effects into the heat conduction analysis. The following conclusions may be drawn.

1. An equivalent loading method was introduced based on the inherent strain. The results indicated that the proposed method was reliable and convenient for predicting the welding deformation during shipbuilding. It can be used to estimate the welding deformation and does not require an elasto-plastic finite element analysis.
2. The inherent strain method that incorporated the hardening effects produced more reliable results than the conventional method. It is therefore essential to incorporate hardening when conducting a welding deformation analysis using the equivalent loading method based on the inherent strain.
3. The proposed method based on the inherent strain could predict the deformation caused when addition loads were added and removed to a structure that had already undergone a thermal history.
4. The conventional inherent strain method was only able to calculate stress levels under the yield stress and could not predict the total deformation in the HAZ after loading and unloading. The proposed method was able to estimate the residual stresses generated by an additional load, even for stress levels over the yield stress, using the deformation analysis process.

Therefore, we can use the proposed inherent strain method to plan how to lift a structure with a HAZ because proposed method makes it possible to predict the deformation generated by the weight of the material and additional loads.

REFERENCES

1. Jang, C. D., Seo, S. I. and Ko, D. E., "A Study on the Prediction of Deformations of Plates Due to Line Heating using a Simplified Thermal Elasto-plastic Analysis," Journal of Ship Production, Vol. 13, No. 1, pp. 22-27, 1997.
2. Jang, C. D., Lee, C. H. and Ko, D. E., "Prediction of Welding Deformations of Stiffened Panels," Journal of Engineering for the Maritime Environment, Vol. 216, No. M2, pp. 133-143, 2002.
3. Ha, Y. S. and Jang, C. D., "An Improved Inherent Strain Analysis for Plate Bending by Line Heating Considering Phase Transformation of Steel," International Journal of Offshore and Polar Engineering, Vol. 17, No. 2, pp. 139-144, 2007.
4. Jang, C. D., Kim, T. H. and Ko, D. E., "Prediction of Steel Plate Deformation Due to Triangle Heating Using Inherent Strain Method," Journal of Marine Science and Technology, Vol. 10, No. 4, pp. 211-216, 2005.
5. Patel, B., "Thermo-Elasto-Plastic Finite Element Formulation for Deformation and Residual Stresses Due to Welds," Ph.D. Thesis, Carleton Univ., 1985.
6. Lee, J. H., Woo, J. H. and Rim, C. W., "Simulation of Multi-Layered Welding Process Using ANSYS," ANSYS User's Conference, pp. 1-11, 2001.
7. Ko, D. E., Jang, C. D., Seo, S. I. and Lee, H. W., "Real Time Simulation of Deformation Due to Line Heating for Automatic Hull Forming System," Journal of the Society of Naval Architects of Korea, Vol. 36, No. 4, pp. 116-127, 1999.
8. Nomoto, T., Ohmori, T. and Satoh, T., "Development of Simulator for Plate Bending by Line Heating," Journal of the Society of Naval Architects of Japan, Vol. 168, pp. 527-535, 1990.
9. Andrews, K. W., "Empirecal Formila for the Calculation of Some Transformation Temperatures," JISI, Vol. 203, pp. 721-727, 1965.
10. Jang, C. D., Ko, D. E., Moon, S. C. and Seo, Y. R., "Simulation of Plate Deformation by Triangle Heating Process," J. of Soc. of Naval Architects of Korea, Vol. 38, No. 4, pp. 66-74, 2001.
11. Jang, C. D., Ko, D. E. and Seo, S. I., "A study on the prediction of Deformation of Plates Due to Line Heating Using a Simplified Thermal Elasto-Plastic Analysis," J. of Ship Production, Vol. 13, No. 1, pp. 22-27, 1997.
12. Jang, C. D., Lee, C. H. and Ko, D. E., "Prediction of welding deformations of stiffened panels," J. Engineering for the Maritime Environment, Vol. 216, No. 2, pp. 133-144, 2002.

13. Koistinen, D. P. and Marburger, R. E., "A General Equation Prescribing the Extent of the Austenite-Martensite Transformation in Pure Iron-Carbon Alloys and Plain Carbon Steels," Acta. Meta., Vol. 7, pp. 59-60, 1959.

14. Marder, A. R. and Krauss, G., "The Morphology of Martensite in Iron Carbon Alloys," Trans. ASM, Vol. 60, pp. 651-660, 1967.

15. Payson, P. and Savage, C. H., "Martensite Reactions in Alloy Steels," Trans. ASM, Vol. 33, pp. 261-275, 1944.

16. Satoh, K., Matsui, S., Terai, K. and Iwamura, Y., "Water-cooling Effect on Angular Distortion caused by the process of Line Heating in Steel Plates," J. of the Society of Naval Architects of Japan, Vol. 126, pp. 445-458, 1969.

17. Satoh, K. and Terasaki, T., "Effect of Welding Conditions on Welding Deformations in Welded Structure Materials," J. of the Japanese Welding Soc., Vol. 45, No. 4, pp. 302-308, 1976.